*Materials Science Forum Vols. 449-452 (2004) pp. 19-24*
*online at http://www.scientific.net*


# Modeling Precipitate Microstructure Evolution in Alloys With First-Principles Energetic Information

V. Vaithyanathan[1], C. Wolverton[2], and L. Q. Chen[1]

[1]Department of Materials Science and Engineering, The Pennsylvania State University, University Park, PA 16802, U.S.A.

[2]Ford Research Laboratory, MD3028/SRL, Dearborn, MI 48121-2053, U.S.A.

**Keywords**: Precipitate morphology, phase-field method, multiscale, first-principles, Al-alloys.

**Abstract.** This short article reports our recent effort to integrate the mesoscale phase-field method with first-principles total energy calculations, linear response theory, as well as mixed-space cluster expansion. A particular example of applying such a multiscale approach to the case of precipitation of semicoherent θ' particles in an Al-matrix is presented.

## Introduction

Precipitation reaction is a fundamental process underlying the development of many engineering alloys such as Al-alloys and Ni-base superalloys. A typical precipitation process involves a solution treatment at a high temperature, quenching of the homogenized solid solution to a lower temperature, and then annealing of the solution within a two-phase field where second-phase particles are thermodynamically expected. The two-phase microstructure, i.e. the size, shape, and distributions of precipitate particles, precipitate volume fraction, as well as the nature (coherent or incoherent) of interfaces between precipitates and matrix play a critical role in the mechanical strength of the two-phase alloy.

Recently, there is an increasing interest to explore computational models that can be employed to predict the precipitate microstructure evolution during aging, and thus have the potential to assist the design of experimental conditions for the desirable mechanical properties. One of the models that received significant attention during the last decade is the phase-field method that has been applied to modeling microstructure evolution for a wide variety of materials processes including precipitation reactions [1]. The phase-field method allows for arbitrary precipitate morphology and a variety of thermodynamic driving forces including bulk chemical free energy, interfacial energy, elastic strain energy, and applied fields. However, phase-field models often rely on empirical or difficult-to-measure physical quantities as input for computing the various energetic contributions to the driving force for microstructure evolution. This is particularly true for Al-alloys in which the most desirable precipitates are metastable and thus their structures and properties are difficult to be determined or measured. On the other hand, density functional calculations, although they are limited to relatively small systems with a few hundred atoms, have shown to be highly accurate in predicting the properties of stable as well as metastable precipitates [2]. Therefore, one of our recent research foci has been on integrating the atomic level state-of-the-art density functional calculations with the mesoscale phase-field approach to predict the precipitate microstructure evolution in alloys. This short article summarizes our recent work in applying such an integrated multiscale approach to the precipitate microstructures of metastable, semicoherent θ' in an Al-matrix [3,4]. We showed that it is possible to calculate many of the input quantities to a phase-field model from atomistic calculations: bulk free energies of solid solution and precipitate phases, interfacial free energies between matrix and precipitate, and coherency strain energies. The incorporation of these energetic properties, obtained from atomistics, into a continuum microstructural model provides the possibility to predict precipitate microstructure evolution starting from first-principles.

## Precipitation Reactions in Al-Alloys

The Al-rich portion of the Al-Cu phase diagram in the solid state consists of a single-phase field of Al-Cu solid solution ($a$) and a two-phase equilibrium of $a$ and the $\theta$-$Al_2Cu$ ordered

intermetallic phase. Although $\theta$ is the thermodynamic equilibrium phase, its appearance during the aging of a Al-Cu solid solution, especially at temperatures below 250°C, is preceded by various metastable precipitates. It is generally believed that the precipitation sequence follows [5]

$$\alpha \rightarrow \alpha + GP \rightarrow \alpha + \theta'' \rightarrow \alpha + \theta' \rightarrow \alpha + \theta \quad (1)$$

where GP represents the Guinier-Preston (GP) zones. θ' and θ" are the intermediate metastable precipitate phases. While GP zones and θ" are coherent, θ' is semi-incoherent, and θ" is incoherent. Experimental measurements of mechanical properties as a function of aging time, temperature, and alloy composition show that the maximum hardness in the temperature range of 190 – 230°C in binary Al-Cu alloys is associated with the presence of θ' precipitates [6]. Therefore, θ' precipitation process has been extensively studied and will also be the focus of discussion of the present article.

## Computational Methodologies

The proposed integration of a number of different computational methodologies is schematically illustrated in Fig.1. First-principles calculations used in this approach are based on the density functional theory within the local density approximation (LDA). For total energy calculations, both the full-potential linearized augmented plane wave method (FLAPW) [7] and the pseudopotential method utilizing ultrasoft pseudopotentials as implemented in the Vienna Simulation Package (VASP) [8] were employed. Vibrational entropies were obtained from linear response calculations [9], which utilized norm-conserving pseudopotentials. The mixed-space cluster expansion (MSCE) technique along with first-principles calculations are used to calculate the energetics of disordered solid solution phases at finite temperatures including the important energetic effects of atomic relaxations [10]. In the MSCE technique, energetics of small unit cell ordered compounds are mapped onto a generalized Ising-like model for a particular lattice type, involving 2-, 3-, and 4-body interactions plus coherency strain energies (atomic misfit strain). Using this Hamiltonian in Monte Carlo simulations, coupled with thermodynamic integration, we can obtain the bulk free energy of the Al-Cu solid solution phase as a function of composition and temperature.

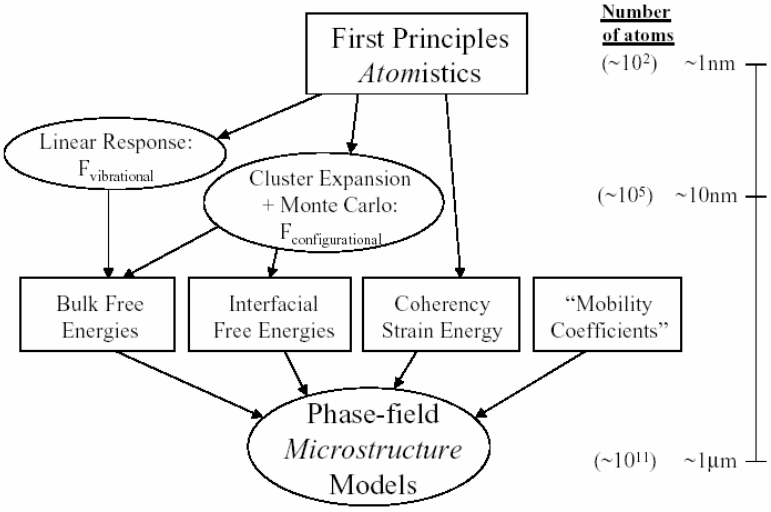


Fig. 1. Schematic of the multiscale model, showng different constituent models and their links along with their associated length scales

The energetic information obtained from the atomistic approaches is then used in a phase-field model in which a precipitate microstructure is described by a set of continuum order parameter fields characterizing the difference in composition and structures between the precipitate and matrix. All the energetic contributions are formulated as functionals of the order parameter fields. The temporal evolution of the microstructure in the phase-field model is obtained by numerically solving the Allen-Cahn and Cahn-Hilliard equations [11,12] for structural fields and composition, respectively.

## Thermodynamic Properties from First Principles

The mixed-space CE Hamiltonian for fcc Al-Cu was constructed from first-principles total energies of 41 ordered structures [2]. Tests were performed to ensure that the first-principles energetics converged with respect to $k$ points (up to a 16x16x16 grid was used) and basis-set cutoffs ($E_{\text{cut}}$ =16.7 and 21.5 $R_{\text{y}}$ were used in the FLAPW and VASP calculations, respectively). The structures, in all cases, were fully relaxed with respect to volume as well as all cell-internal and -external coordinates. The MC simulations using MSCE Hamiltonian constructed from first-principles energetics, provide the total system energy per atom ($E_{\text{SS}}$) as a function of absolute temperature for different solute (Cu) compositions. The free energies (in meV/atom) as a function of composition and temperature, obtained from first-principles atomistics, are shown in Fig. 2

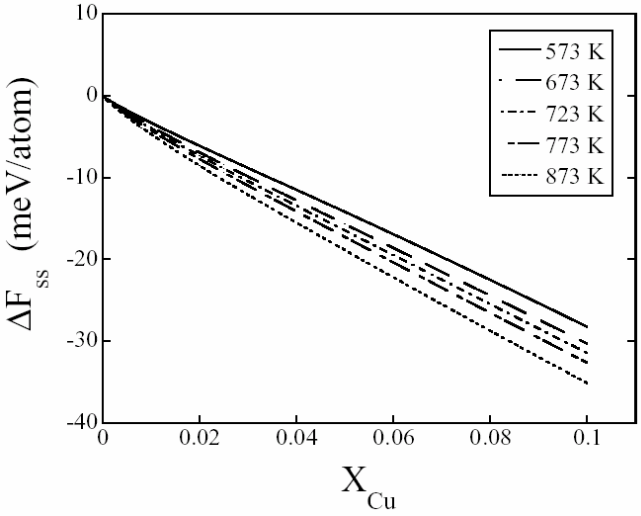


Fig. 2. Free energy of the Al-Cu solid solution as a function of composition and temperature, calculated using the first-principles, cluster expansion, MC and thermodynamic integration.

We treat $\theta'$ as a line compound. The energy of the $\theta'$ metastable phase is obtained from direct first-principles calculations at $T$=0 K. With the vibrational entropy of $\theta'$ [9], the free energy of $\theta'$ as a function of temperature is given by,

$$\Delta F_{\theta'}(T) = -195.8 + 0.62 k_B T \left(\text{in } meV/atom\right). \quad (2)$$

The interfacial energies are obtained from VASP calculations of supercell energies by subtracting the bulk energies of $\theta'$ and Al. Supercells with 24 to 120 atoms were used, with the large supercell results demonstrating that the energies are well converged with respect to supercell size. The calculated T=0 K interfacial energies from first-principles LDA calculations for coherent and semi-coherent interfaces are ~ 190 and 600 mJ/m$^2$, respectively. These values provide an interfacial energy anisotropy of ~3 which is significantly different from prior theoretical estimates of Aaronson and Laird [13] which gave rise to an interfacial energy anisotropy of ~12.

The elastic constants of cubic ($CaF_2$ structure) $\theta'$ were calculated via FLAPW: $C_{11}$=1.9 Mbar, $C_{12}$=0.8 Mbar and $C_{44}$=0.9 Mbar.

The equilibrium or stress-free T=0 K lattice parameters for pure fcc Al and $\theta'$-$Al_2Cu$ calculated using first-principles (FLAPW-LDA) are $a_{Al} = 0.3989nm, a_{\theta'} = 0.4019nm, c_{\theta'} = 0.5684nm$ . By examining a number of different possibilities, it is shown that a $2c_{\theta'} \mid 3a_{Al}$ configuration for the semi-coherent interface between $\theta'$ and Al generates the least lattice deformation, consistent with the experimental observation by Stobbs and Purdy [14]. With the above lattice parameters from first-principles, the lattice misfits are determined to be +0.68% and -5.1% for the coherent and semi-coherent interfaces, respectively.

**Phase-Field Modeling**

All the energetic contributions to a $Al-\theta'$ microstructure from first-principles atomistic calculations are incorporated in a phase-field model. The example presented here assumes the local free energy as a function of both composition and structural order parameter fields and the coefficients in the free energy model are fitted to the free energies of Al solid solution and the $\theta'$ precipitates obtained from first-principles. More details of the free energy function can be

found in references [3,4]. Based on the free energy, and we chose the gradient energy coefficients to produce the same interfacial energies as those calculated from the first-principles [3,4].

The elastic energy is evaluated using the Khachaturyan's elasticity theory [15] by assuming that the local transformation strain, i.e. the stress-free strain associated with the cubic to tetragonal theta' transformation, is proportional to the square of local structural order parameter values [16].

The coupled Allen-Cahn [11] and Cahn-Hilliard equations [12] are solved using the semi-implicit Fourier Spectral method [17] to yield the temporal and spatial evolution of composition and structural order parameter fields, and thus the $\theta'$ microstructure evolution.

Based on the bulk free energy and the interfacial energy, the estimate for interfacial width of the coherent interface is ~1.2 nm. The grid spacing $\Delta x$ is chosen as 0.5 nm. Alternative phase-field formulations may be able to artificially increase the interfacial width to allow larger grid size, but with increasing complexity in solving the phase-field equations [18]. While the 3D simulations can be performed and is on-going, this short article summarizes our work on 2D because of the computational limitations involved in modeling a realistic system size in 3D. In 2D, the plate-shaped $\theta'$ precipitates will be modeled as if viewed edge-on and the number of orientation variants will be 2. The 2D simulation sizes were ~ 750 $nm^2$.

**Morphological Evolution of $\theta'$**

The precipitate growth and coarsening as a function of time for 2 at% is shown in Fig.3. Based on the relationship between physical parameters and those used in the phase-field model, the time in the simulation may be converted to real time.

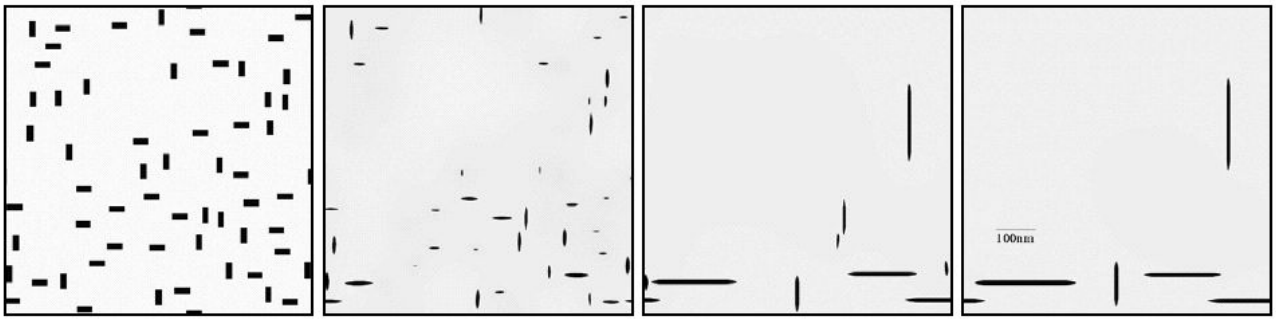


Fig. 3. Microstructure evolution as a function of dimensionless time ($t^*$) for Al-2 at% Cu alloy. The simulation size is ~750 $nm^2$

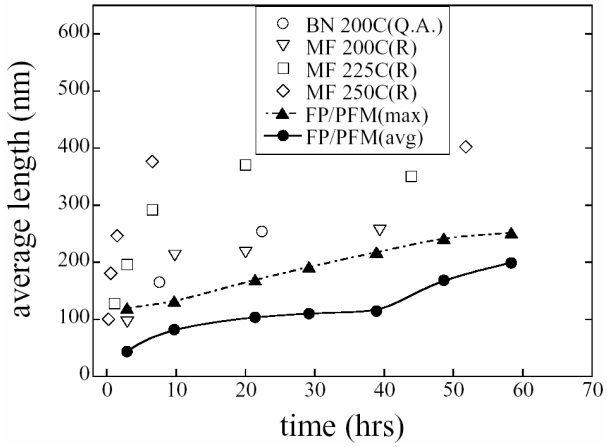


Fig. 4. Average and maximum precipitate length for Al-2 at% Cu alloy: our simulation (FP/PFM), experiments of BN [19] and MF [20]. `Q.A.' represents quenching and aging while `R' represents reversion treatment.

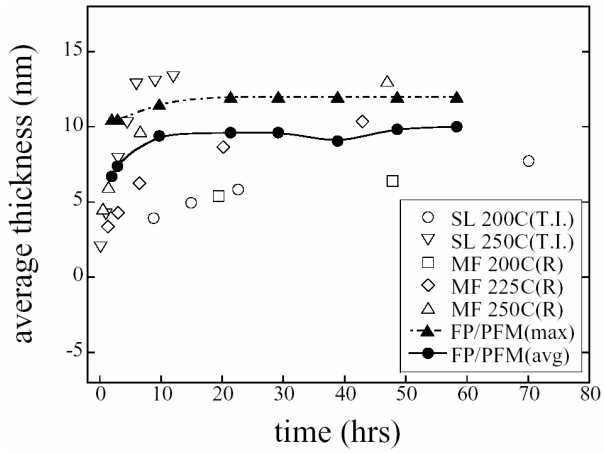


Fig. 5. Average and maximum precipitate thickness for Al-2 at% Cu alloy: our simulation (FP/PFM), experiments of SL [21] and MF [20]. `T.I.' represents isothermal treatment

From the microstructure evolution in Fig. 3, quantitative precipitate features such as the thickness, length and aspect ratio are extracted as a function of time. The thickening and lengthening kinetics obtained from Al-2 at% Cu alloy are shown in Fig. 4 and Fig. 5. It should be emphasized that the number of precipitates is small in the simulation, so the statistics is poor. Furthermore, the simulations were performed in 2D. Therefore, the comparisons between the simulation and experiments are still qualitative. The simulation results are compared with the experimental measurements available for precipitation temperatures between 200 and 250°C. The average (solid line) and maximum (dotted line) values of length and thickness from the simulation are compared with those from the experiments. From Fig. 4 and Fig. 5, it is clear that the thickness values from simulation are in closer agreement with experimental results, as compared to the precipitate length. The main reason is the fact that no kinetic anisotropy was included in the present simulation. Work is in progress to incorporate the kinetic effect on the lengthening kinetics. The average aspect ratio of $\theta'$ precipitates in the 2 at%Cu alloy is ~20 from the late stages of microstructure evolution (Fig. 6). Merle and Fouquet [20] obtained similar aspect ratios after long aging times (few hundred to thousand hours). Based on the interfacial energy anisotropy from first-principles calculations, the equilibrium aspect ratio of $\theta'$ precipitate should be close to 3, when the precipitate shape is purely controlled by the interfacial energy. The large aspect ratios of $\theta'$ precipitates observed experimentally even after long aging times (~20) could be reasoned with two arguments. The first is the possibility that even after long aging time, the precipitate shapes never reach equilibrium, i.e., the non-equilibrium aspect ratio induced by interfacial kinetic anisotropy persists or the equilibrium shape of the precipitates could also be controlled by elastic energy anisotropy. The simulation results on equilibrium precipitate morphology show that the combination of interfacial energy and elastic energy anisotropy can result in precipitate aspect ratios much larger than 3. Therefore, the equilibrium precipitate morphology is governed

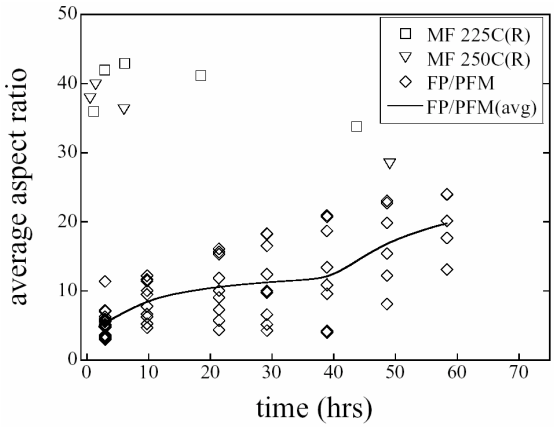


Fig. 6. Average aspect ratio compared with the experimental results of MF [20]. The individual aspect ratios from the simulation (FP/PFM) are displayed along with the average aspect ratio in solid line atom

not just by the interfacial energy anisotropy as it has been previously believed, but by a combination of the ``interfacial and elastic energy anisotropies''. It is generally agreed that the aspect ratios of 40 and above observed for theta' precipitates is a result of the kinetic anisotropy (lengthening to thickening kinetics).

**Summary**

A multiscale approach is presented for studying the precipitate morphology of $\theta'$ precipitates in Al-Cu alloys. Energetics required by the mesoscale phase-field are provided by atomistics first-principles calculations combined with cluster expansion and MC techniques. First-principles calculations provide the first reliable interfacial energy and misfit strain values for the coherent and semi-coherent interfaces of $\theta'$. From the multiscale simulation results, we show that the average equilibrium aspect ratio resulting from this anisotropy combination can be much larger than that determined from the interfacial energy anisotropy alone. The time evolution of the precipitate features such as the length, thickness, and aspect ratio predicted by the simulation agrees qualitatively with the experimental observations. It is expected that quantitative agreement with experiment is possible by incorporating the non-equilibrium interfacial mobility anisotropy effect and by performing large-scale simulations in 3D.

**Acknowledgments:** The work is supported by Ford Motor Company through a University Research Project and partially by the NSF under the grant number DMR01-22638

**References**

[1] L. Q. Chen, Ann. Rev. of Mater. Res. Vol. 32 (2002), p113.
[2] C. Wolverton. Phil. Mag. Lett. Vol. 79 (1999), p683.
[3] V. Vaithyanathan, C. Wolverton, and L. Q. Chen. Phys. Rev. Lett. Vol. 88 (2002), p125503.
[4] V. Vaithyanathan, C. Wolverton, and L. Q. Chen. Acta Mater., to be submitted, (2003).
[5] G. W. Lorimer, In: Precipitation processes in solid. Russel KC, Aaronson HI, editors. TMS AIME, 1978, p87.
[6] H. K. Hardy. J. Inst. Metals Vol. 79, (1951) p321, 1951; ibid, Vol. 82 (1953), p 236.
[7] D. J. Singh. Planewaves, Pseudopotentials, and the LAPW Method. Kluwer, Boston, 1994.
[8] G. Kresse and J. Furthmuller. Comput. Mater. Sci. Vol. 6 (1996), p15.
[9] C. Wolverton and V. Ozolins. Phys. Rev. Lett. Vol. 8 (2001), p5518.
[10] D. B. Laks, L. G. Ferreira, S. Froyen, and A. Zunger. Phys. Rev. B Vol. 46 (1992), p12587.
[11] Allen, S. M. and J. W. Cahn, Journal de Physique Vol. C7 (1977), p51.
[12] Cahn, J. W., "On Spinodal Decomposition." Acta Metall. Vol. 9 (1961), p795.
[13] H. I. Aaronson and C. Laird. Ford Motor Co. Scientific Laboratory Report, 1967.
[14] W. M. Stobbs and G. R. Purdy. Acta Metall. Vol. 26 (1978), p1069.
[15] A. G. Khachaturyan and V. G. Hairapetyan. Phys. Stat. Sol. (b) Vol. 57 (1973), p801.
[16] Chen, L. Q., Y. Z. Wang, et al. Phil. Mag. Lett. Vol. 65 (1992), p15.
[17] L. Q. Chen and J. Shen. Comp. Phys. Comm. Vol. 108 (1998), p147.
[18] Kim, S. G., W. T. Kim, et al., Phys. Rev. E Vol. 60 (1999), p7186.
[19] J. D. Boyd and R. B. Nicholson. Acta Metall. Vol 19 (1971), p1379.
[20] P. Merle and F. Fouquet. Acta Metall. Vol. 29 (1981), p1919.
[21] R. Sankaran and C. Laird. Acta Metall. Vol. 22 (1974), p957.